

Local structure of vanadium in doped LiFePO_4

Ting Zhao,^a Wei Xu,^a Qing Ye,^a Jie Cheng,^a Haifeng Zhao,^a Ziyu Wu,^{a,b,*}
Dingguo Xia^{c,*} and Wangsheng Chu^{a,*}

^aInstitute of High Energy Physics, Chinese Academy of Sciences, Beijing 100049, People's Republic of China, ^bNational Synchrotron Radiation Laboratory, University of Science and Technology of China, Hefei 230026, People's Republic of China, and ^cCollege of Engineering, Peking University, Beijing 100871, People's Republic of China. E-mail: wuzy@ustc.edu.cn, dgxia@bjut.edu.cn, cws@ihep.ac.cn

LiFePO_4 composites with 5 at.% vanadium doping are prepared by solid state reactions. X-ray absorption fine-structure spectroscopy is used as a novel technique to identify vanadium sites. Both experimental analyses and theoretical simulations show that vanadium does not enter into the LiFePO_4 crystal lattice. When the vanadium concentration is lower than 1 at.%, the dopant remains insoluble. Thus, a single-phase vanadium-doped LiFePO_4 cannot be formed and the improved electrochemical properties of vanadium-doped LiFePO_4 previously reported cannot be associated with crystal structure changes of the LiFePO_4 via vanadium doping.

© 2010 International Union of Crystallography
Printed in Singapore – all rights reserved

Keywords: lithium-ion battery; LiFePO_4 ; XAFS; vanadium; doping site.

1. Introduction

As a type of energy storage device characterized by the advantage of low maintenance costs, negligible self-discharge, high energy density and no memory effects, lithium-ion batteries are becoming more and more popular in technological applications from wireless communications to mobile computing. The key issue for the development of lithium-ion batteries is the electrode materials. Although the commercial use of LiCoO_2 has already gained great success, further large-scale applications of lithium-ion batteries in the future (e.g. in hybrid electric vehicles) demand for a cheaper cathode material. Lithium iron phosphate (LiFePO_4), proposed by Padhi *et al.* (1997), is one of the most promising candidates not only because of its potential low cost but also for its environmental benignancy and structural stability. However, in the almost perfect framework its bottleneck is represented by the low intrinsic electrical conductivity (Jugovic & Uskokovic, 2009). Several approaches have been explored to overcome the conductivity problem. These approaches include the reduction of the particle size, the achievement of a homogeneous particle size distribution (Gaberscek *et al.*, 2007), particles coated with carbon (Franger *et al.*, 2006; Song *et al.*, 2007), and doping with supervalent cations to enhance the intrinsic conductivity (Chung *et al.*, 2002; Ravet *et al.*, 2003; Wagemaker *et al.*, 2008; Meethong *et al.*, 2009).

Recently, a composite of LiFePO_4 with $\text{Li}_3\text{V}_2(\text{PO}_4)_3$ addition was prepared (Wang *et al.*, 2008; Choi & Kumta, 2007), and both electrical conductivity and high-rate discharge capacity were improved. Later, both Sun *et al.* (2009) and

Hong *et al.* (2009) reported an enhancement of electrochemical performances of the single-phase vanadium-doped LiFePO_4 . However, structural evidence for the vanadium substitution was still incomplete. X-ray diffraction (XRD) analysis is not sufficient for characterizing these materials because this technique is sensitive to crystalline systems and amorphous impurities such as Fe_2O_3 in LiFePO_4 are not detectable (Liu *et al.*, 2009). In addition, XRD patterns of complex compounds show several intense peaks that may easily cover the contribution of impurities, particularly when their content is low. This is probably the inconsistency present in the contribution of Sun *et al.* (2009) where doped vanadium atoms replace iron atoms and in the contribution of Hong *et al.* (2009) where vanadium atoms occupy phosphor sites.

Synchrotron-radiation-based X-ray absorption fine-structure (XAFS) spectroscopy is a powerful spectroscopic tool that provides detailed information regarding the local geometry and the electronic structure of the investigated materials. Previous XAFS investigations have been performed on lithium-ion batteries (Wu *et al.*, 1996; Deb *et al.*, 2004; Kobayashi *et al.*, 2004). Owing to the elemental specificity and detection sensitivity, XAFS is a unique tool for characterizing the aliovalent doping in LiFePO_4 . In this contribution we apply both X-ray absorption near-edge spectroscopy (XANES) and extended X-ray absorption fine-structure (EXAFS) spectroscopy to identify whether vanadium atoms get inside the crystal lattice of LiFePO_4 , and furthermore to investigate what is the existing form of vanadium in the doped LiFePO_4 .

2. Experimental section

2.1. Materials and experimental conditions

Vanadium-doped LiFePO_4 samples were synthesized by solid state reactions. The raw materials, Li_2CO_3 , $\text{FeC}_2\text{O}_4 \cdot 2\text{H}_2\text{O}$, $\text{NH}_4\text{H}_2\text{PO}_4$ and NH_4VO_3 , were thoroughly mixed together in stoichiometric ratios for the target compounds (e.g. $\text{Li}:\text{Fe}:\text{P}:\text{V} = 1.00:1.00:0.95:0.05$ for $\text{LiFeP}_{0.95}\text{V}_{0.05}\text{O}_4$) and then ball-milled for 3 h in acetone. After being dried, the mixture was heated at 623 K for 3 h to be pre-decomposed, and subsequently sintered at 973 K for 9 h under a flowing gas mixture (5% H_2 in Ar). Crystalline phases of the obtained materials were analyzed by XRD using a D8 Advance X-ray diffractometer working with $\text{Cu K}\alpha$ radiation over an angular 2θ range from 10 to 90° . V_2O_3 and VO_2 standard samples were bought from Fisher Scientific (USA), V_2O_5 from Tianjin Kermel Chemical Reagent company (China), while $\text{Li}_3\text{V}_2(\text{PO}_4)_3$ was prepared by methods described elsewhere (Rui *et al.*, 2009).

2.2. XAFS measurements

2.2.1. Fe K-edge XAFS measurements. X-ray absorption spectra at the Fe K-edge were collected in transmission mode at the U7C beamline of the National Synchrotron Radiation Laboratory (NSRL) from 200 eV below up to 800 eV above the Fe K absorption edge (7112 eV). The storage ring was working at 800 MeV and experiments were performed at room temperature with an electron current decreasing from 200 to 100 mA during a time span of about 12 h. Si (111) crystals were used to monochromatize the X-rays and to reduce higher harmonics; the second crystal was detuned by about 30%. The intensities of the incident and the transmitted X-rays were monitored by ionization chambers filled with nitrogen and helium gas mixtures.

2.2.2. V K-edge XAFS measurements. X-ray absorption spectra at the V K-edge were obtained at the X-ray absorption station of the 1W1B beamline at the Beijing Synchrotron Radiation Facility (BSRF) in the same relative energy range as the Fe K-edge. Standard samples of V_2O_3 , VO_2 , V_2O_5 and $\text{Li}_3\text{V}_2(\text{PO}_4)_3$ were recorded in transmission mode while the prepared doped samples were measured in fluorescence mode. The typical energy of the storage ring was 2.5 GeV with the current decreasing from 250 to 150 mA during a time span of about 8 h. Also a Si (111) double-crystal monochromator was used with a detuning of about 50% at the V K-edge.

3. Results and discussion

3.1. Crystalline phases of $\text{LiFeP}_{0.95}\text{V}_{0.05}\text{O}_4$ and $\text{LiFe}_{0.95}\text{V}_{0.05}\text{PO}_4$

For both Fe and P sites, 5 at.% vanadium atoms were considered in LiFePO_4 . XRD patterns of doped $\text{LiFeP}_{0.95}\text{V}_{0.05}\text{O}_4$ and $\text{LiFe}_{0.95}\text{V}_{0.05}\text{PO}_4$ compounds together with that of the undoped LiFePO_4 are compared in Fig. 1. For the pure LiFePO_4 sample all diffraction peaks can be indexed assuming an orthorhombic structure and space group $Pnma$.

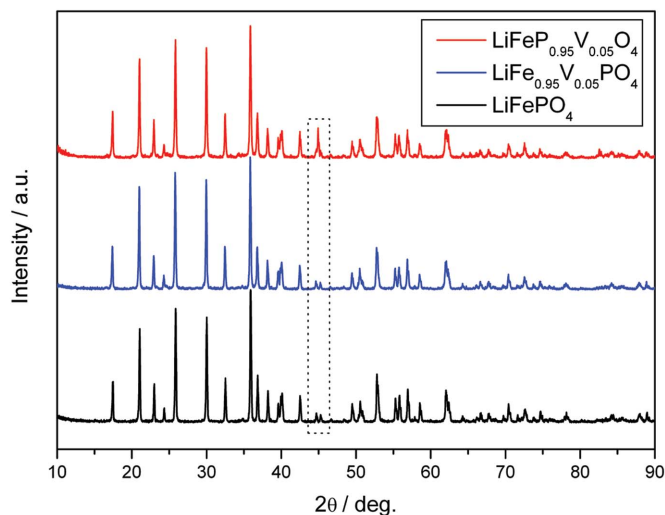


Figure 1
X-ray diffraction patterns of $\text{LiFeP}_{0.95}\text{V}_{0.05}\text{O}_4$, $\text{LiFe}_{0.95}\text{V}_{0.05}\text{PO}_4$ and pure LiFePO_4 samples.

For $\text{LiFe}_{0.95}\text{V}_{0.05}\text{PO}_4$, as also found by Sun *et al.* (2009), XRD patterns do not show any impurity phase peaks. On the contrary, in the spectrum of $\text{LiFeP}_{0.95}\text{V}_{0.05}\text{O}_4$, a clear peak from an impurity phase appears at about 45° (see the dashed rectangle in Fig. 1). This impurity phase cannot be identified owing to the high intensity of the main peaks.

3.2. XANES and EXAFS analysis of $\text{LiFeP}_{0.95}\text{V}_{0.05}\text{O}_4$ and $\text{LiFe}_{0.95}\text{V}_{0.05}\text{PO}_4$

Fe K-edge XANES data for $\text{LiFeP}_{0.95}\text{V}_{0.05}\text{O}_4$, $\text{LiFe}_{0.95}\text{V}_{0.05}\text{PO}_4$ and pure LiFePO_4 are compared in Fig. 2. Within the tolerance of the signal-to-noise ratio, the spectra of doped $\text{LiFe}_{0.95}\text{V}_{0.05}\text{PO}_4$ and pure LiFePO_4 appear identical, indicating a similar local structure around the Fe sites. On the contrary, visible differences exist in the main peak and in the pre-peak between the data of $\text{LiFeP}_{0.95}\text{V}_{0.05}\text{O}_4$ and pure LiFePO_4 . Considering that the XRD patterns of

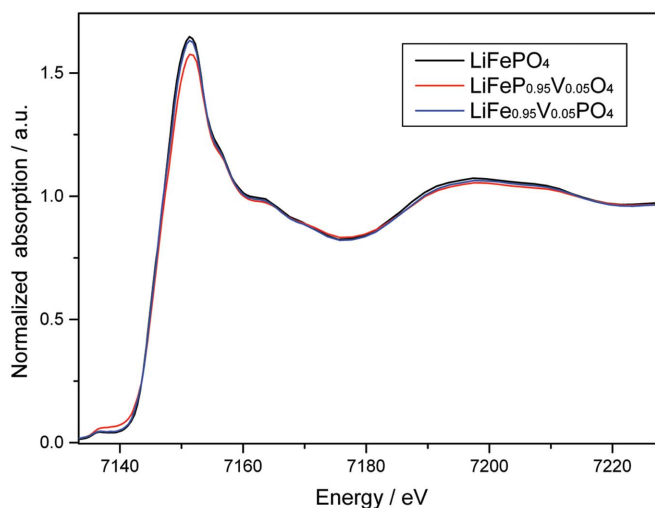


Figure 2
Comparison of normalized Fe K-edge XANES spectra of $\text{LiFeP}_{0.95}\text{V}_{0.05}\text{O}_4$, $\text{LiFe}_{0.95}\text{V}_{0.05}\text{PO}_4$ and pure LiFePO_4 samples.

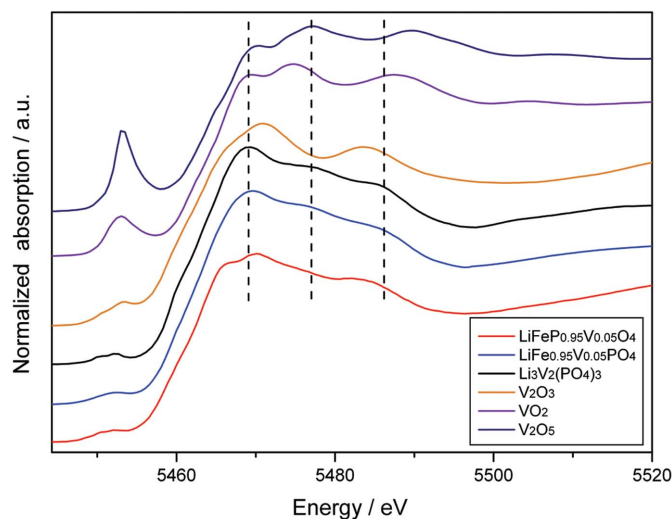


Figure 3
V *K*-edge XANES spectra of $\text{LiFeP}_{0.95}\text{V}_{0.05}\text{O}_4$ and $\text{LiFe}_{0.95}\text{V}_{0.05}\text{PO}_4$ samples and of reference materials such as $\text{Li}_3\text{V}_2(\text{PO}_4)_3$, V_2O_3 , VO_2 and V_2O_5 .

$\text{LiFeP}_{0.95}\text{V}_{0.05}\text{O}_4$ show the presence of an impurity phase, we may claim that in the case of $\text{LiFeP}_{0.95}\text{V}_{0.05}\text{O}_4$ vanadium atoms do not enter inside the crystal lattice of LiFePO_4 leading to a relative excess of iron, while forming another iron compound compatible with the differences observed in the XANES spectra at the Fe *K*-edge.

Direct information regarding vanadium in $\text{LiFeP}_{0.95}\text{V}_{0.05}\text{O}_4$ and in $\text{LiFe}_{0.95}\text{V}_{0.05}\text{PO}_4$ is given by the V *K*-edge XANES data shown in Fig. 3. XANES structures originating from multiple-scattering processes of the photoelectrons with neighbouring atoms return details about the electronic structure and the local arrangement of atoms around the V absorbing atom. Looking at Fig. 3, the XANES of V_2O_3 , VO_2 , V_2O_5 and $\text{Li}_3\text{V}_2(\text{PO}_4)_3$ show clear differences owing to their different chemical constitutions, and the XANES of the well known chemical constituents provide useful standards for recognizing unknown chemical forms such as V atoms in the doped LiFePO_4 . In the literature, the vanadium oxidation state is determined through the position of the absorption near edge, which shifts to higher energies with increasing valence state. In our study the absorption edge increases from about 5454.5 eV to 5458.2 eV as the valence state of vanadium shifts from +3 in V_2O_3 to +5 in V_2O_5 . Because the absorption edge is at 5454.3 eV, the valence state of vanadium in $\text{LiFe}_{0.95}\text{V}_{0.05}\text{PO}_4$ may be assigned to +3, while vanadium in $\text{LiFeP}_{0.95}\text{V}_{0.05}\text{O}_4$ has a lower valence state for the absorption edge at 5453.5 eV. The XANES features of $\text{LiFe}_{0.95}\text{V}_{0.05}\text{PO}_4$ and $\text{LiFeP}_{0.95}\text{V}_{0.05}\text{O}_4$ also show large differences. As a consequence, different stoichiometric ratios largely affect the existing form of vanadium. The pre-edge peak corresponding to the $1s \rightarrow 3d$ transition is a clear fingerprint of the symmetry and can be used to evaluate qualitatively changes of the vanadium local symmetry. Symmetrical vanadium–ligand coordinations with inversion symmetry, such as a regular ‘ VO_6 ’ octahedral environment in the VO compound, have negligible pre-edge intensities (Silversmit *et al.*, 2006). In contrast, coordinations without

inversion symmetry, such as distorted ‘ VO_6 ’ units in V_2O_3 and in VO_2 or the ‘ VO_4 ’ tetrahedral coordinations in NH_4VO_3 , show significant to large pre-edge intensities (Silversmit *et al.*, 2005; Wu & Xian, 2001). In the case of $\text{LiFeP}_{0.95}\text{V}_{0.05}\text{O}_4$, if vanadium atoms are located at P sites a large pre-edge intensity may appear because phosphorus atoms share a tetrahedron geometry with the surrounding oxygen atoms in the LiFePO_4 crystal. However, XANES data of $\text{LiFeP}_{0.95}\text{V}_{0.05}\text{O}_4$ in Fig. 3 show only a small pre-edge peak, not in agreement with the vanadium substitution at P sites.

To extract detailed structural information around the absorbing vanadium atoms, XANES simulations were performed in the framework of the multiple-scattering theory (Lee & Pendry, 1975; Natoli *et al.*, 1990) using the *FEFF8.2* code (Ankudinov *et al.*, 1998). V *K*-edge XANES calculations were performed with the structural model and lattice parameters of the host structure, *i.e.* olivine LiFePO_4 (García-Moreno *et al.*, 2001), in which a V atom replaces P and Fe in $\text{LiFeP}_{0.95}\text{V}_{0.05}\text{O}_4$ and $\text{LiFe}_{0.95}\text{V}_{0.05}\text{PO}_4$, respectively. The *FEFF* input file was generated by the *ATOMS* package and the cluster potential was approximated by a set of spherically averaged muffin-tin potentials. For the calculations a model cluster including all atoms within 5 Å of the central V atom was constructed for the self-consistent field potential calculations, and a cluster with a radius of 7 Å was used for full multiple-scattering calculations. Calculation results and experimental data are compared in Fig. 4. Clear discrepancies can be recognized in the relative peak intensities and peak positions for both $\text{LiFeP}_{0.95}\text{V}_{0.05}\text{O}_4$ and $\text{LiFe}_{0.95}\text{V}_{0.05}\text{PO}_4$. Data suggest that vanadium atoms do not enter the selected sites in both $\text{LiFeP}_{0.95}\text{V}_{0.05}\text{O}_4$ and $\text{LiFe}_{0.95}\text{V}_{0.05}\text{PO}_4$.

To compare XANES spectral features we set three vertical dashed lines in Fig. 3 as guides for the eye. From the comparison the spectral profile of $\text{LiFe}_{0.95}\text{V}_{0.05}\text{PO}_4$ appears quite similar to that of $\text{Li}_3\text{V}_2(\text{PO}_4)_3$, a behaviour consistent with the presence of the vanadium inside $\text{LiFe}_{0.95}\text{V}_{0.05}\text{PO}_4$ and in agreement with EXAFS data. Looking at Fig. 5, the EXAFS signal of $\text{LiFe}_{0.95}\text{V}_{0.05}\text{PO}_4$ shows great differences with that of the pure LiFePO_4 , whereas a good correspondence occurs between the structures of $\text{LiFe}_{0.95}\text{V}_{0.05}\text{PO}_4$ and $\text{Li}_3\text{V}_2(\text{PO}_4)_3$. In the case of $\text{LiFeP}_{0.95}\text{V}_{0.05}\text{O}_4$ the presence of vanadium cannot be recognized by a qualitative comparison of XAFS data *via* a linear combination of reference spectra owing to the lack of reference systems.

3.3. XANES and EXAFS analysis of $\text{LiFeP}_{0.99}\text{V}_{0.01}\text{O}_4$ and $\text{LiFe}_{0.99}\text{V}_{0.01}\text{PO}_4$

The insolubility of 5 at.% vanadium doped in LiFePO_4 at both Fe and P sites may be due to the high doping level. Studies were then focused on samples with a lower vanadium concentration such as $\text{LiFeP}_{0.99}\text{V}_{0.01}\text{O}_4$ and $\text{LiFe}_{0.99}\text{V}_{0.01}\text{PO}_4$ samples. XRD patterns of these samples display a single LiFePO_4 phase (Fig. 6) and may barely provide any useful information about the local environment of vanadium. Moreover, XANES data in Fig. 7 show that the spectrum of $\text{LiFeP}_{0.99}\text{V}_{0.01}\text{O}_4$ as well as that of $\text{LiFe}_{0.99}\text{V}_{0.01}\text{PO}_4$ has a weak

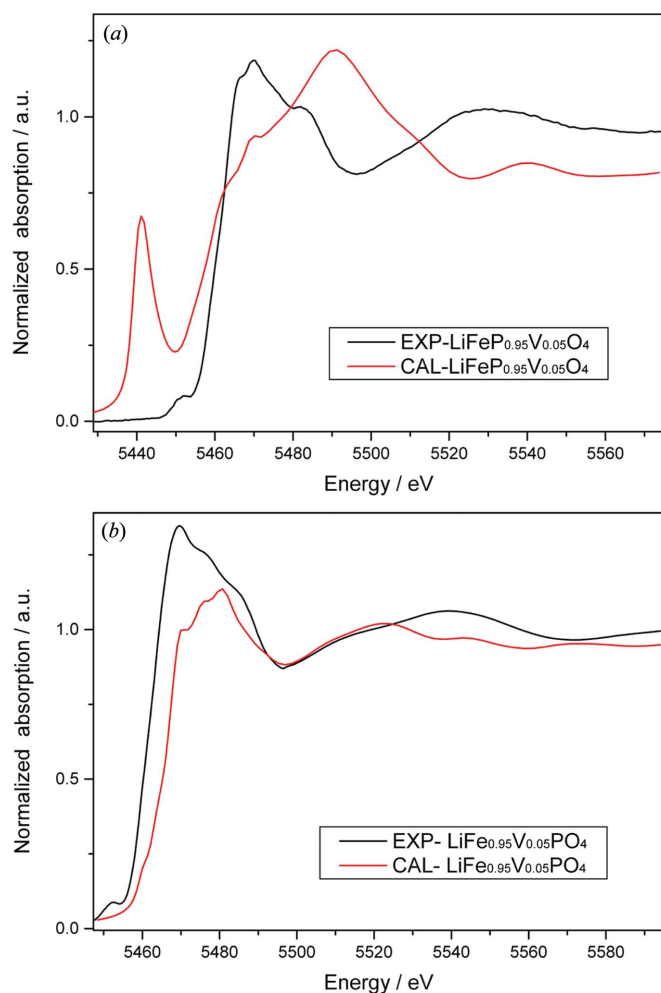


Figure 4
Comparison of theoretical calculations (CAL) and experimental spectra (EXP) of $\text{LiFeP}_{0.95}\text{V}_{0.05}\text{O}_4$ (a) and $\text{LiFe}_{0.95}\text{V}_{0.05}\text{PO}_4$ (b).

pre-edge peak that suggests a ‘ VO_6 ’ octahedral environment. They show a great similarity with $\text{Li}_3\text{V}_2(\text{PO}_4)_3$. The data show that in these two low-level doped samples vanadium forms a $\text{Li}_3\text{V}_2(\text{PO}_4)_3$ phase, a hypothesis supported by the analogy of the EXAFS spectra shown in Fig. 8.

4. Conclusions

In this study, LiFePO_4 samples were synthesized *via* solid state reactions to achieve vanadium doping at both Fe and P sites. The solubility of vanadium was investigated by the XAFS technique. XANES theoretical simulations at the V *K*-edge show large deviations from experimental spectra, providing reliable evidence of the insolubility of vanadium in LiFePO_4 . XANES and EXAFS experiments confirm that vanadium in doped samples of Fe sites is consistent with the $\text{Li}_3\text{V}_2(\text{PO}_4)_3$ composition. On the contrary, that in doped samples of P sites appears to show filling a VO_6 octahedral environment although a definite chemical configuration has not been determined. Also, at lower dopant concentrations, for example, at 1 at.%, vanadium does not select Fe and P sites in

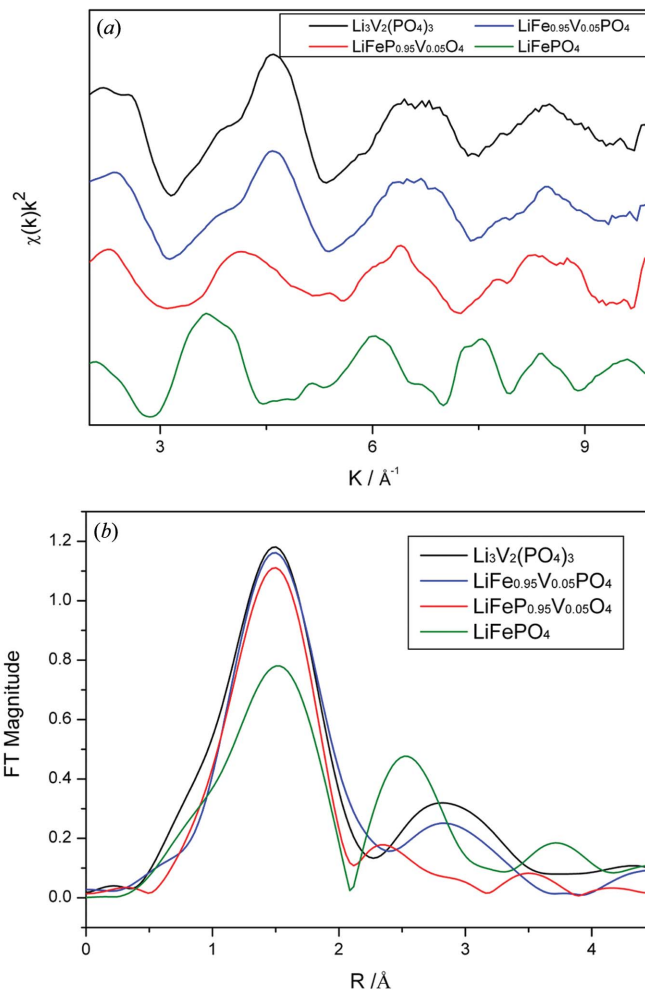


Figure 5
(a) k^2 -extracted EXAFS signals in the range 2–10 \AA^{-1} at the Fe *K*-edge for pure LiFePO_4 and at the V *K*-edge for $\text{LiFe}_{0.95}\text{V}_{0.05}\text{PO}_4$, $\text{LiFeP}_{0.95}\text{V}_{0.05}\text{O}_4$ and $\text{Li}_3\text{V}_2(\text{PO}_4)_3$ samples; (b) the corresponding radial structure functions in *r*-space.

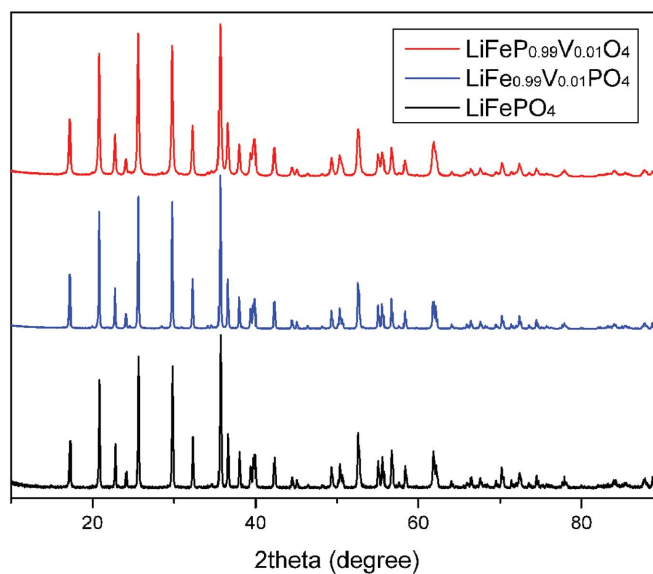


Figure 6
X-ray diffraction patterns of $\text{LiFeP}_{0.99}\text{V}_{0.01}\text{O}_4$, $\text{LiFe}_{0.99}\text{V}_{0.01}\text{PO}_4$ and pure LiFePO_4 samples.

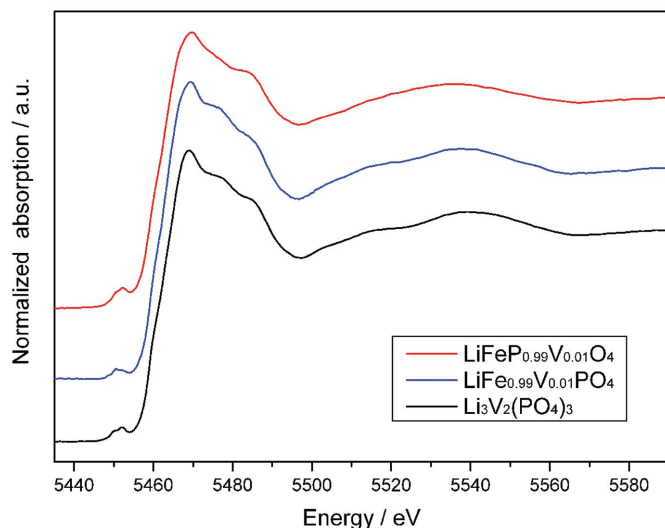


Figure 7
V K-edge XANES spectra of $\text{LiFeP}_{0.99}\text{V}_{0.01}\text{O}_4$, $\text{LiFe}_{0.99}\text{V}_{0.01}\text{PO}_4$ and $\text{Li}_3\text{V}_2(\text{PO}_4)_3$ samples.

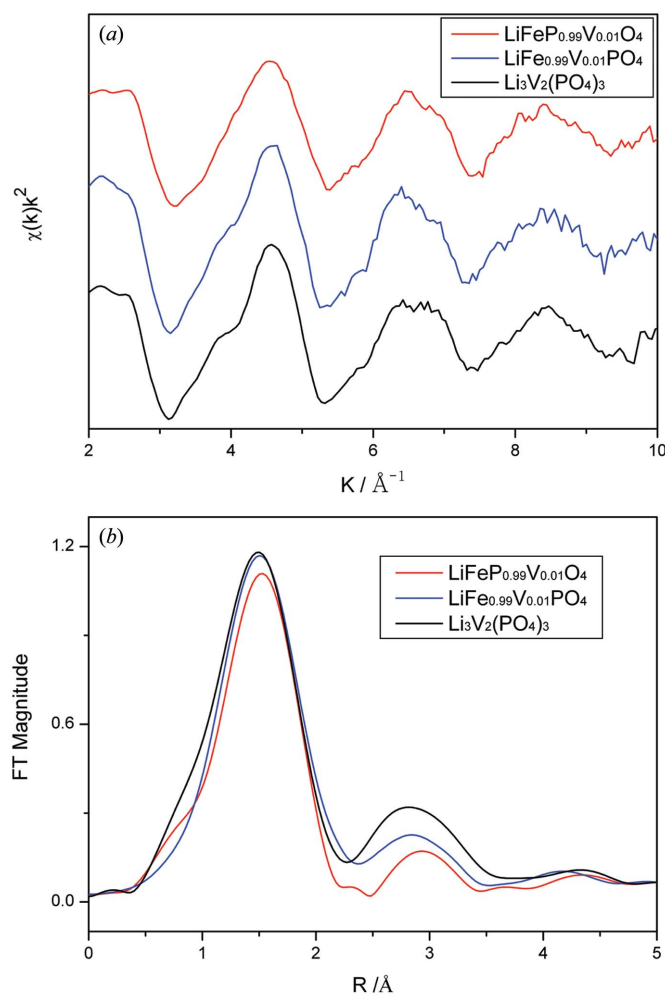


Figure 8
Comparison of k^2 -extracted V K-edge EXAFS signals in k -space (a) and r -space (b) for $\text{LiFeP}_{0.99}\text{V}_{0.01}\text{O}_4$, $\text{LiFe}_{0.99}\text{V}_{0.01}\text{PO}_4$ and $\text{Li}_3\text{V}_2(\text{PO}_4)_3$ samples.

the crystal lattice of LiFePO_4 while forming a $\text{Li}_3\text{V}_2(\text{PO}_4)_3$ phase. Actually, this study provides a new reliable method of investigating doped LiFePO_4 materials. Structural information associated with a dopant barely distinguished in an XRD pattern may be revealed by the XAFS analysis. However, further work is necessary to build up a clear framework regarding the doping of transition metal elements in LiFePO_4 . The results achieved also point out that the method can be applied to investigate other doped electrode systems.

The above analysis clearly shows that enhanced electrochemical performances of the LiFePO_4 composite following vanadium addition cannot be due to a crystal structural change of the LiFePO_4 . Alternatively, mechanisms suggested by Wang *et al.* (2008) and Choi & Kumta (2007) should be considered. In addition, the deviation from the stoichiometry of LiFePO_4 that may induce the presence of secondary phases such as $\text{Fe}_2\text{P}/\text{Fe}_3\text{P}$ may also contribute to the observed enhanced conductivity (Subramanya Herle *et al.*, 2004; Kang & Ceder, 2009). An accurate investigation with other technical means is under way to give the exact mechanism.

This work was partly supported by the National Outstanding Youth Fund (Project No. 10125523 to ZW), the Knowledge Innovation Program of the Chinese Academy of Sciences (KJCX2- YW-N42), the Natural Science Foundation for the Youth (10805055) and the National Natural Science Foundation of China (Y01139005C).

References

Ankudinov, A. L., Ravel, B., Rehr, J. J. & Conradson, S. D. (1998). *Phys. Rev. B*, **58**, 7565–7576.

Choi, D. & Kumta, P. N. (2007). *J. Power Sources*, **163**, 1064–1069.

Chung, S.-Y., Bloking, J. T. & Chiang, Y.-M. (2002). *Nat. Mater.* **1**, 123–128.

Deb, A., Bergmann, U., Cairns, E. J. & Cramer, S. P. (2004). *J. Synchrotron Rad.* **11**, 497–504.

Franger, S., Benoit, C., Bourbon, C. & Le Cras, F. (2006). *J. Phys. Chem. Solids*, **67**, 1338–1342.

Gaberscek, M., Dominko, R. & Jamnik, J. (2007). *Electrochem. Commun.* **9**, 2778–2783.

Garcia-Moreno, O., Alvarez-Vega, M., Garcia-Alvarado, F., Garcia-Jaca, J., Gallardo Amores, J. M., Sanjuan, M. L. & Amador, U. J. (2001). *Mater. Chem.* **13**, 1570–1576.

Hong, J., Wang, C. S., Chen, X., Upreti, S. & Stanley Whittingham, M. (2009). *Electrochem. Solid-State Lett.* **12**, A33–A38.

Jugovic, D. & Uskokovic, D. (2009). *J. Power Sources*, **190**, 538–544.

Kang, B. & Ceder, G. (2009). *Nature (London)*, **458**, 190–193.

Kobayashi, S., Usui, T., Ikuta, H., Uchimoto, Y. & Wakihara, M. (2004). *J. Am. Ceram. Soc.* **87**, 1002–1004.

Lee, P. A. & Pendry, J. B. (1975). *Phys. Rev. B*, **11**, 2795–2811.

Liu, J., Jiang, R., Wang, X., Huang, T. & Yu, A. (2009). *J. Power Sources*, **194**, 536–540.

Meethong, N., Kao, Y.-H., Speakman, S. A. & Chiang, Y.-M. (2009). *Adv. Funct. Mater.* **19**, 1060–1070.

Natoli, C. R., Benfatto, M., Brouder, C., López, M. F. R. & Foulis, D. L. (1990). *Phys. Rev. B*, **42**, 1944–1968.

Padhi, A. K., Nanjundaswamy, K. S. & Goodenough, J. B. (1997). *J. Electrochem. Soc.* **144**, 1188–1194.

- Ravet, N., Abouimrane, A. & Armand, M. (2003). *Nat. Mater.* **2**, 702–703.
- Rui, X. H., Li, C. & Chen, C. H. (2009). *Electrochim. Acta*, **54**, 3374–3380.
- Silversmit, G., Poelman, H., Sack, I., Buyle, G., Marin, G. B. & De Gryse, R. (2006). *Catal. Lett.* **107**, 61–71.
- Silversmit, G., van Bokhoven, J. A., Poelman, H., van der Eerden, A. M. J., Marin, G. B., Reyniers, M.-F. & De Gryse, R. (2005). *Appl. Catal. A*, **285**, 151–162.
- Song, M.-S., Kang, Y.-M., Kim, J.-H., Kim, H.-S., Kim, D.-Y., Kwon, H.-S. Lee, J.-Y. (2007). *J. Power Sources*, **166**, 260–265.
- Subramanya Herle, P., Ellis, B., Coombs, N. & Nazar, L. F. (2004). *Nat. Mater.* **3**, 147–152.
- Sun, C. S., Zhou, Z., Xu, Z. G., Wang, D. G., Wei, J. P., Bian, X. K. & Yan, J. (2009). *J. Power Sources*, **193**, 841–845.
- Wagemaker, M., Ellis, B. L., Lutzenkirchen-Hecht, D., Mulder, F. M. & Nazar, L. F. (2008). *Chem. Mater.* **20**, 6313–6315.
- Wang, L. N., Li, Z. C., Xu, H. J. & Zhang, K. L. (2008). *J. Phys. Chem. C*, **112**, 308.
- Wu, Z. & Xian, D. C. (2001). *Appl. Phys. Lett.* **79**, 1918.
- Wu, Z. Y., Ouvrard, G., Lemaux, S., Moreau, P., Gressier, P., Lemoigno, F. & Rouxel, J. (1996). *Phys. Rev. Lett.* **77**, 2101–2104.